



Scholars Research Library

Der Pharma Chemica, 2015, 7(2):301-306
(<http://derpharmachemica.com/archive.html>)



ISSN 0975-413X
CODEN (USA): PCHHAX

New eco-friendly corrosion inhibitor: Inhibitive and adsorption action of clay for the corrosion of stainless steel in H_3PO_4 solutions

M. Boudalia¹, A. Guenbour¹, A. Bellaouchou¹ and A. Zarrouk²

¹Laboratoire de Nanotechnologie, d'Electrochimie-Corrosion, Matériaux et environnement-
Faculté des Sciences, Université Mohamed V, Av. Ibn Batouta, Rabat, Morocco

²LCAE-URAC18, Faculté des Sciences, Université Mohammed Premier, Oujda, Morocco

ABSTARCT

The corrosion inhibition of stainless steel in 5.5 M H_3PO_4 by clay has been studied as a possible source of eco-friendly inhibitor using potentiodynamic polarization curves and electrochemical impedance spectroscopy (EIS) methods at 298 K. Results obtained showed that this clay functioned as a corrosion inhibitor for stainless steel in the acidic environment. Inhibition efficiency increased with clay concentration. Polarization curves indicate that this inhibitor acts as a cathodic inhibitor. EIS spectra exhibit one capacitive loop. The charge transfer resistance (R_{ct}) increases with inhibitor concentration, while double layer capacitance (C_{dl}) decreases. Adsorption of this inhibitor on stainless steel surface obeys the Langmuir adsorption isotherm.

Keywords: Stainless steel, Phosphoric acid, Clay, Electrochemical techniques.

INTRODUCTION

The corrosion of metallic materials in acidic solutions causes considerable costs. Several techniques have been applied to reduce metal corrosion. The use of inhibitors during acid pickling is a practical protection method against corrosion in acidic media. Most effective and efficient organic inhibitors are compounds containing heteroatoms, such as oxygen, nitrogen, sulfur, and phosphorus, which allow adsorption on metal surfaces [1-19].

Inorganic inhibitors are also used to secure metals against corrosion; we cite molybdate, vanadate, halides as well as metallic ions as Zn^{2+} , Cu^{2+} , and Ce^{3+} ... [20-22].

Though many organic and inorganic compounds show good anticorrosive activity, most of them are highly toxic to both human beings and environment. The investigation of new non-toxic or low-toxic and green corrosion inhibitors is essential to overcome this problem. In the 21st Century, the research in the field of "green" or "eco-friendly" corrosion inhibitors has been addressed toward the goal of using cheap, effective molecules at low or "zero" environmental impact. Up to now, many alternative eco-friendly organic and inorganic inhibitors have been developed [23].

This study aims to investigate the inhibitory effect of clay, an affordable, ecofriendly, and naturally occurring substance, on the corrosion of stainless steel in a 5.5 M H_3PO_4 solution through potentiodynamic polarisation curves and electrochemical impedance spectroscopy (EIS) methods. The adsorption of clay was investigated.

MATERIALS AND METHODS

Materials

The steel used in this study is a UB6 stainless steels with a chemical composition (in wt%) of 4.39 % Mo, 0.0013 % C, 1.45 % Si, 1.84 % Mn, 0.007 % S, 20.77 % Cr, 0.0029 % P, 25.09 % Ni, 2.36CU % Others and the remainder iron (Fe).

Solutions

The electrolyte used in this study was (5.5M) 40% H_3PO_4 contaminated with addition of 4% of H_2SO_4 and 400 ppm of chloride ions. In this last case, the solution was called polluted H_3PO_4 solution. The concentrations of clay are 0.002 g/L, 0.004 g/L, 0.006 g/L and 0.008 g/L.

Electrochemical measurements

The electrochemical study was carried out using a potentiostat PGZ100 piloted by Voltmaster software. This potentiostat is connected to a cell with three electrode thermostats a saturated calomel electrode (SCE) and platinum electrode were used as reference and auxiliary electrodes, respectively. The working electrode is a circular shaped and the exposed area of the specimen to the solution was 0.67cm^2 . Anodic and cathodic potentiodynamic polarization curves were plotted at a polarization scan rate of 0.5 mV/s .

The experiments were conducted under thermostated conditions at 298 K. Before the potentiostatic passivation experiments, the surface of the samples was cleaned cathodically at -0.6 V/SCE for 15 minutes. The working electrode was polarised for 1 hour at the different temperatures. The electrochemical impedance spectroscopy (EIS) measurements are carried after potentiostatic passivation tests. After the determination of steady-state current at a corrosion potential, sine wave voltage (10 mV) peak to peak, at frequencies between 100 kHz and 100 mHz. The impedance diagrams are given in the Nyquist representation.

RESULTS AND DISCUSSION

Potentiodynamic Polarization Study

It is well established that polarization curves can help to understand how a certain corrosion inhibitor works. Inhibitors can modify the anodic process, the cathodic process or both leading to a decreased rate of the global corrosion process. Fig. 1 shows typical polarization curves for stainless steel carried in aerated 5.5 M H_3PO_4 in the absence and presence of varied concentrations of clay. In the figure, two important trends are evident. Firstly, that this inhibitor is found to block the electrochemical processes taking place on the stainless steel undergoing corrosion in phosphoric acid solutions. It reduces both the rate of cathodic and anodic reactions by reducing the current densities on both sides of the polarization curves in the potential region studied and hence reduces the corrosion rate. Secondly, it shifts the open corrosion potentials towards more negative values with reference to the blank. These factors suggest that this inhibitor acts as cathodic type corrosion inhibitor [24-26].

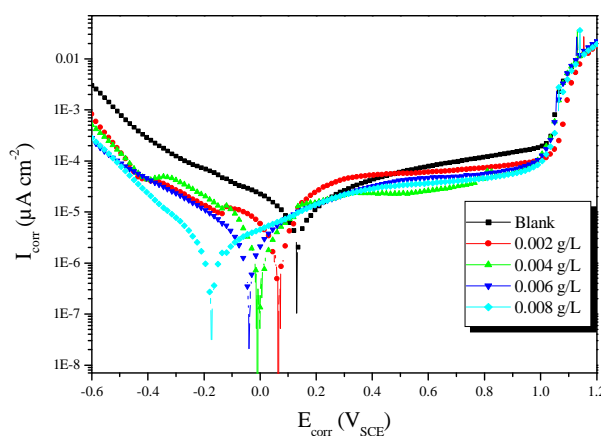


Figure 1. Polarisation curves of stainless steel in 5.5 M H_3PO_4 at different concentrations of clay

The data obtained from polarization curves by Tafel extrapolations are presented in Table 1. These include corrosion potential (E_{corr}), corrosion current density (I_{corr}), cathodic and anodic Tafel slopes (β_c and β_a) at varied clay concentrations. Correspondingly, IE% increases with the inhibitor concentration, due to the increase in the blocked fraction of the electrode surface by adsorption. IE% of 0.008 g/L inhibitor reaches up to the maximum of 88%, which indicates that clay is a good inhibitor for stainless steel in 5.5 M H_3PO_4 . The potentiodynamic curves show that there is a clear reduction of both the anodic and cathodic currents in the presence of clay compared with those for the blank solution. It is clear that the cathodic reaction (hydrogen evolution) and the anodic reaction (dissolution metal) were inhibited. The values of cathodic Tafel slope β_c in the presence of inhibitor was changing, which clearly indicates that this inhibitor influence the kinetics of hydrogen evolution reaction. This indicates an increase in the energy barrier for proton discharge leading to less gas evolution. The values of η_p (%) increased with increase in concentration of inhibitor, which indicates higher surface coverage of the metal. It can be seen from Table 1 that the corrosion potential, E_{corr} , becomes more negative as the concentration increases.

The linear Tafel segments of anodic and cathodic curves were extrapolated to corrosion potential to obtain corrosion current densities (I_{corr}). From the polarization curves obtained, the corrosion current (I_{corr}) was calculated by curve fitting using the equation:

$$I = I_{\text{corr}} \left[\exp\left(\frac{2.3\Delta E}{\beta_a}\right) - \exp\left(\frac{2.3\Delta E}{\beta_c}\right) \right] \quad (1)$$

The inhibition efficiency was evaluated from the measured I_{corr} values using the relationship:

$$\eta_p \% = \frac{I_{\text{corr}}^{\circ} - I_{\text{corr}}^i}{I_{\text{corr}}^{\circ}} \times 100 \quad (2)$$

where, I_{corr}° and I_{corr}^i are the corrosion current density in absence and presence of inhibitor, respectively.

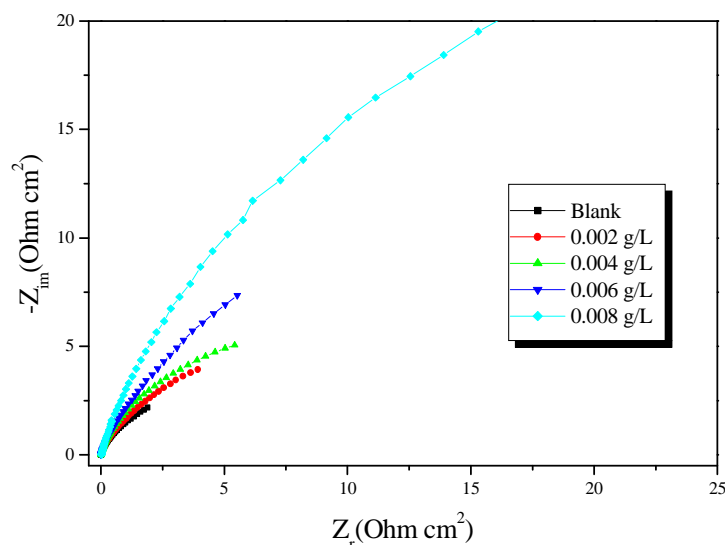
Table 1. Polarisation data of carbon steel in 5.5 M H_3PO_4 without and with addition of inhibitor at 298 K

| | Conc | E_{corr} (mV/SCE) | β_a (mV/dec) | $-\beta_c$ (mV/dec) | I_{corr} ($\mu\text{A}/\text{cm}^2$) | η_p (%) |
|-------|-----------|-------------------------------|-----------------------|---------------------|--|-----------------|
| Blank | 5.5 M | 132 | 380.4 | 306.2 | 41.9 | ---- |
| | 0.002 g/L | 63.3 | 404.8 | 207.1 | 13.2 | 68 |
| Clay | 0.004 g/L | -43.1 | 230.7 | 347.6 | 10.4 | 75 |
| | 0.006 g/L | -9.2 | 290.1 | 263.7 | 8.0 | 81 |
| | 0.008 g/L | -177.1 | 341.5 | 288.0 | 5.0 | 88 |

Electrochemical impedance spectroscopy

The inhibition process of the gum exudates was also studied by electrochemical impedance spectroscopy technique. Impedance measurements in the Nyquist format for stainless steel exposed for 1 hour in the acidic solutions containing different concentrations of the clay. The impedance behavior of stainless steel in 5.5 M H_3PO_4 with and without addition of various concentrations of clay is presented as complex impedance plot (Nyquist plot) in Fig. 2. It is seen from this figure that the presence of the clay in the phosphoric acid solutions leads to changes of the impedance diagram in both shape and size.

It is clear from this figure that the impedance diagrams are not perfect semicircles reported to be attributed to the frequency dispersion [27]. The size of the capacitive arc increased with increase in inhibitor concentrations up to 0.008 g/L. This suggests that, 0.008 g/L could be considered as the optimum inhibitor concentration forming the optimum protective film on the substrate surface against the charge transfer.



The impedance spectra for different Nyquist plots were analyzed using a Complex Nonlinear Least Squares (CNLS) fitting program, EQUIVCRT and the equivalent circuit model and relevant relations used are described elsewhere [28]. The values of elements fitted the model, that is, charge transfer resistances (R_{ct}) and that of double layer capacitances (C_{dl}) calculated are listed in Table 2. The table also includes the open circuit potential, calculated corrosion rates and percentage inhibitor efficiency (η_z %). Since, the corrosion rate is inversely proportional to the charge transfer; η_z % was calculated by use of the relation given above. It is seen from this table that as inhibitor concentration increases, the R_{ct} values increase while the double-layer capacitance decreases. This indicates that, clay is corrosion inhibitive. The decrease in the C_{dl} values in the presence of the clay shows that clay adsorbs on the metal surface and forms a film that reduces the metal surface area undergoing corrosion. It has been reported that the adsorption process on the metal surface is characterized by a decrease in C_{dl} [29]. The inhibition efficiencies obtained by impedance studies are in agreement with those obtained employing potentiodynamic polarization technique.

The inhibition efficiency of the inhibitor was calculated from the charge transfer resistance values using the following equation [30]:

$$\eta_z \% = \frac{R_{ct(inh)} - R_{ct}}{R_{ct(inh)}} \times 100 \quad (3)$$

where R_{ct} and $R_{ct(inh)}$ were the values of polarization resistance in the absence and presence of inhibitor, respectively.

Table 2. Electrochemical impedance parameters and inhibition efficiency for stainless steel in 5.5 M H_3PO_4 solution with clay at 298K

| | Conc | R_{ct} (Ω cm^2) | C_{dl} ($\mu F/cm^2$) | η_z (%) |
|-------|-----------|---------------------------------|------------------------------|-----------------|
| Blank | 5.5 M | 204.0 | 173.8 | ---- |
| Clay | 0.002 g/L | 587.4 | 192.3 | 65.0 |
| | 0.004 g/L | 732.7 | 166.5 | 73.0 |
| | 0.006 g/L | 912.1 | 102.0 | 78.0 |
| | 0.008 g/L | 990.0 | 74.5 | 80.3 |

Adsorption isotherm

The efficiency of inhibitor molecules are related to their adsorption ability on the metal surface. An inhibitor reduces the corrosion rate by covering active centers on the metal surface. So, it is important to determine surface coverage ratio value (θ) for discussing the corrosion rate properly. The value is simply obtained from inhibition efficiency values,

$\theta = \eta_z/100$. In Fig. 3, the linear relationships of C/θ versus C suggest that the adsorption of clay on the stainless steel is in well agreement with the Langmuir adsorption isotherm, which is expressed by the following equation [31].

$$\frac{C_{inh}}{\theta} = \frac{1}{K_{ads}} + C_{inh} \quad (4)$$

where C_{in} is inhibitor concentration and K_{ads} is the adsorption equilibrium constant for the adsorption-desorption process. The K_{ads} value was obtained from the intercept of plot. The agreement with the Langmuir isotherm shows that the inhibitor adsorption is physical. This isotherm supposes that adsorbed molecules constitute a monolayer on the surface, but the intermolecular attractions are inevitable between the adsorbed molecules and other near by the surface. Therefore the obtained efficiencies are sensible against inhibitor concentration.

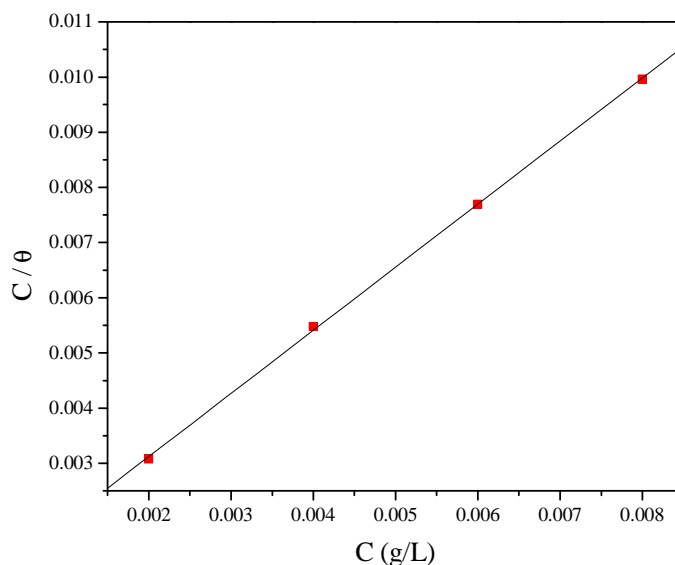


Figure 3. Langmuir adsorption of clay on the stainless steel surface in 5.5 H_3PO_4 solution

CONCLUSION

The polarization studies showed that clay is a cathodic-type inhibitor of corrosion one that decreases both cathodic hydrogen reduction reactions and anodic metal dissolution and that its corrosion efficiency increased with the inhibitor concentration. AC impedance results showed that charge transfer resistance increases with increase in the clay concentration. The adsorption isotherm of clay on the stainless steel in 5.5 M H_3PO_4 solution obeyed Langmuir adsorption isotherm with high correlation coefficient. The results obtained from different experimental studies are in good agreement.

REFERENCES

- [1] A. K. Singh, M. A. Quraishi, *J. Mater. Environ. Sci.* **2010**, 1, 101.
- [2] U.J. Naik, V.A. Panchal, A.S. Patel, N.K. Shah, *J. Mater. Environ. Sci.* **2012**, 3, 935.
- [3] A. Zarrouk, B. Hammouti, H. Zarrok, R. Salghi, A. Dafali, Lh. Bazzi, L. Bammou, S. S. Al-Deyab, *Der Pharm. Chem.* **2012**, 4, 337.
- [4] A. Zarrouk, B. Hammouti, H. Zarrok, S.S. Al-Deyab, M. Messali, *Int. J. Electrochem. Sci.* **2011**, 6, 6261.
- [5] H. Zarrok, R. Saddik, H. Oudda, B. Hammouti, A. El Midaoui, A. Zarrouk, N. Benchat, M. Ebn Touhami, *Der Pharm. Chem.* **2011**, 3, 272.
- [6] D. Ben Hmamou, R. Salghi, A. Zarrouk, B. Hammouti, S.S. Al-Deyab, Lh. Bazzi, H. Zarrok, A. Chakir, L. Bammou, *Int. J. Electrochem. Sci.* **2012**, 7, 2361.
- [7] A. Zarrouk, B. Hammouti, A. Dafali, H. Zarrok, *Der Pharm. Chem.* **2011**, 3, 266.
- [8] A. Ghazoui, R. Saddik, N. Benchat, B. Hammouti, M. Guenbour, A. Zarrouk, M. Ramdani, *Der Pharm. Chem.* **2012**, 4, 352.
- [9] A. Zarrouk, B. Hammouti, H. Zarrok, I. Warad, M. Bouachrine, *Der Pharm. Chem.* **2011**, 3, 263.
- [10] A. H. Al Hamzi, H. Zarrok, A. Zarrouk, R. Salghi, B. Hammouti, S. S. Al-Deyab, M. Bouachrine, A. Amine, F. Guenoun, *Int. J. Electrochem. Sci.* **2013**, 8, 2586.

- [11] A. Ghazoui, N. Bencat, S. S. Al-Deyab, A. Zarrouk, B. Hammouti, M. Ramdani, M. Guenbour, *Int. J. Electrochem. Sci.* **2013**, 8, 2272.
- [12] D. Ben Hmamou, R. Salghi, A. Zarrouk, M. Messali, H. Zarrok, M. Errami, B. Hammouti, Lh. Bazzi, A. Chakir, *Der Pharm. Chem.* **2012**, 4, 1496.
- [13] A. Zarrouk, H. Zarrok, R. Salghi, N. Bouroumane, B. Hammouti, S. S. Al-Deyab, R. Touzani, *Int. J. Electrochem. Sci.* **2012**, 7, 10215.
- [14] H. Bendaha, A. Zarrouk, A. Aouniti, B. Hammouti, S. El Kadiri, R. Salghi, R. Touzani, *Phys. Chem. News*, **2012**, 64, 95.
- [15] A. Zarrouk, B. Hammouti, H. Zarrok, M. Bouachrine, K.F. Khaled, S.S. Al-Deyab, *Int. J. Electrochem. Sci.* **2012**, 6, 89.
- [16] S. Rekkab, H. Zarrok, R. Salghi, A. Zarrouk, Lh. Bazzi, B. Hammouti, Z. Kabouche, R. Touzani, M. Zougagh, *J. Mater. Environ. Sci.* **2012**, 3, 613.
- [17] A. Ghazoui, R. Saddik, N. Bencat, M. Guenbour, B. Hammouti, S.S. Al-Deyab, A. Zarrouk, *Int. J. Electrochem. Sci.* **2012**, 7, 7080.
- [18] H. Zarrok, A. Zarrouk, R. Salghi, Y. Ramli, B. Hammouti, M. Assouag, E. M. Essassi, H. Oudda and M. Taleb, *J. Chem. Pharm. Res.* **2012**, 4, 5048.
- [19] H. Zarrok, K. Al Mamari, A. Zarrouk, R. Salghi, B. Hammouti, S. S. Al-Deyab, E. M. Essassi, F. Bentiss, H. Oudda, *Int. J. Electrochem. Sci.* **2012**, 7, 10338.
- [20] G.N. Mu, X.H. Li, Q. Qu, J. Zhou, *Acta Chim. Sinica*, **2004**, 62, 2386.
- [21] M.A. Deyab, S.S. Abd El-Rehim, *Electrochim. Acta*, **2007**, 53, 1754.
- [22] M. Saremi, C. Dehghanian, M.M. Sabet, *Corros. Sci.* **2006**, 48, 1404.
- [23] A. Tizpar, Z. Ghasemi, *Appl. Surf. Sci.* 2006, **252**, 8630.
- [24] S. Bahri, M. Belayachi, H. Zarrok, A. Shaim, M. Galai, A. Zarrouk, A. El Midaoui, M. Ebn Touhami, B. Lakhrissi, H. Oudda, *Der Pharm. Chem.* **2014**, 6, 110.
- [25] M. Larouj, Y. ELaoufir, H. Serrar, A. El Assyry, M. Galai, A. Zarrouk, B. Hammouti, A. Guenbour, A. El Midaoui, S. Boukhriss, M. Ebn Touhami, H. Oudda, *Der Pharm. Lett.* **2014**, 6, 324.
- [26] A. Zarrouk, B. Hammouti, A. Dafali, H. Zarrok, R. Touzani, M. Bouachrine, M. Zertoubi, *Res. Chem. Intermed.* **2012**, 38, 1079.
- [27] K. Juttner, *Electrochim. Acta*, **1990**, 35, 1501.
- [28] J.Y.N. Philip, J. Buchweishaija, L.L. Mkayula, *Tanz. J. Sci.* **2001**, 27, 9.
- [29] A.M. Abdel-Gaber, B.A. Abd-El Nabey, I.M. Sidahmed, A.M. El-Zayady, M. Saadawy, *Corrosion*, **2006**, 62, 293.
- [30] M. Larif, A. Elmidaoui, A. Zarrouk, H. Zarrok, R. Salghi, B. Hammouti, H. Oudda, F. Bentiss, *Res. Chem. Intermed.*, **2012** DOI 10.1007/s11164-012-0788-2.
- [31] J.O'M. Bockris, A.K.N. Reddy, M. Gamboa-Aldeco, *Modern Electrochemistry, second ed.*, Kluwer Academic/Plenum Publishers, New York, **2000**.